

Demonstrable and anatomy-driven knuckle identification via crease map segmentation

Ritesh Vyas^{1*}, Bryan Williams^{2*}, Hossein Rahmani²,
Richard Boswell-Challand², Zheheng Jiang³, Plamen Angelov²,
Sue Black⁴

¹School of Technology, Pandit Deendayal Energy University,
Gandhinagar, 382007, Gujarat, India.

²School of Computing and Communications, Lancaster University,
Lancaster, LA1 4YW, UK.

³University of Leicester, Leicester, LE1 7RH, UK.

⁴St John's College, St Giles, Oxford, OX1 3JP, UK.

*Corresponding author(s). E-mail(s): ritesh.vyas157@gmail.com;
b.williams6@lancaster.ac.uk;

Abstract

Images of the human hand can be effectively deployed to assist with the identification of the perpetrators of serious crimes. One of the prominent and distinguishing features of the human hand is found in the skin of the finger knuckle regions, which includes creases forming complex and distinctive patterns. Exploiting knuckle skin crease patterning in the identification of perpetrators requires manual labelling from expert anthropologists, which is both laborious and time-consuming. Existing approaches for automatic knuckle recognition work in a black-box manner without explicitly revealing the causes of a match or no match. Whereas, the court-room proceedings demand amore transparent and reproduciblematching procedure driven from anatomy and comparison of skin creases. Hence, development of automated algorithms to segment (trace) the knuckle creases and compare them exclusively can make the whole process demonstrable and convincing. This paper proposes an effective framework for knuckle crease identification that can directly work on full hand dorsal images to (i) localize the knuckle regions effectively, (ii) segment (trace) the knuckle creases and (iii) effectively compare knuckles through the segmented crease maps. The novel matching of knuckle creases is achieved through explicit comparison of the creases themselves and is investigated with a large public dataset to demonstrate the potential of the proposed approach.

Keywords: Knuckle crease segmentation, Tracing, Demonstrable

1 Introduction

The finger knuckles, viewed from the dorsal side of the human hand, have shown potential to be used as a biometric trait [1]. All three types of finger knuckles formed on the proximal interphalangeal (PIP), distal interphalangeal (DIP) and metacarpophalangeal (MCP) joints can be utilized for identification of human subjects [2]. However, their potential to provide sufficiently discernible and distinctive features may vary. Several feature descriptors have been developed to represent the knuckle features effectively [3–7]. These descriptors were mainly derived from traditional mechanisms, such as Gabor filters [5], phase-only correlation [6] and the Radon transform [3, 4].

These descriptors have been effectively used to provide features of the knuckle image as a whole, but they fail to provide a comparison which is anatomy-driven and demonstrable. In other words, the above descriptors largely work in a black-box matching scenario. When it comes to the application of forensic science in using knuckle image matching for court-room proceedings, it becomes extremely important to demonstrate the manner of matching between samples of evidence and the suspect. Forensic experts use scientific techniques for perpetrator identification and favour techniques which are transparent and possible to replicate [8]. In other words, if the identification process is not demonstrable in the criminal court or if the defence expert cannot repeat it, their legal team can request it to be dismissed. Therefore, there is a strong demand for the development of transparent and explainable finger knuckle matching techniques which can be used effectively in practice.

To tackle this issue, this work presents a first-of-its kind knuckle crease segmentation approach, which facilitates transparency and demonstration of knuckle crease matching. Kumar and Wang [8] proposed a method for segmenting finger knuckles using a conventional approach of binarization, median filtering, morphological dilation/erosion and thinning. However, due to the dependency on multiple underlying sub-operations and dependence on empirically selected parameters, their approach is unlikely to generalize well. Besides, their approach is tested only with a finger dorsal dataset instead of a full hand-dorsal dataset, where the process deals with the images acquired under highly controlled conditions making it sensitive to variations in hand pose. Hence, we propose a more generalizable approach for knuckle crease segmentation using a data-driven machine learning approach which can handle full hand dorsal images.

Figure 1 illustrates the overall framework of the proposed demonstrable knuckle matching approach. The approach commences with the localization of knuckle region from the input hand dorsal image. It then deals with the knuckle crease segmentation, where the localized knuckle regions are processed for segmenting (tracing) the skin creases using fine-tuned deep learning-based segmentation models. Thereafter, a crease thinning step is performed to obtain the centerline, followed by a detailed

analysis of the performance metrics pertaining to the region segmentation and centerline detection. Subsequently, the obtained centerlines of knuckle skin creases from the gallery and query images are registered to enhance their possible overlap which in turn aids the matching process to determine whether it was a genuine or imposter match.

The two key terminologies (i.e., demonstrability and anatomy-driven nature) of the proposed approach arise from the imperative need of the court-room proceedings to demonstrate the reliability of any source of evidence. The jury/judges in any criminal proceedings do not admit expert evidence unless there are good grounds for believing that the evidence is reliable [9]. Further, knuckle crease matching usually requires humongous efforts from expert anthropologists to present as evidence in order to ascertain the identity of a perpetrator. Hence, any automated method can only prove admissible in the court-room proceedings, if they are backed by the anatomical information.

1.1 Contributions

The major contributions of this work are listed as follows:

- A novel framework for segmenting the knuckle creases and establishing identity from them is presented.
- This is the first work to achieve a generalizable segmentation of the knuckle creases and explicitly investigate demonstrable knuckle crease matching with a large public dataset.
- The crease segmentation results are validated through an expert anthropologist and numerical evaluation is given through segmentation and centerline metrics.

The rest of the paper is organized in the following way: Sect. 2 explains the proposed methodology to achieve the knuckle crease segmentation and crease-matching, Sect. 3 constitutes the details about datasets, experimental setup, performance metrics and the results, and finally the paper concludes in Sect. 4.

2 Proposed methodology

The proposed matching algorithm largely builds upon the appropriateness of the crease segmentation. Therefore, the key steps of crease segmentation are illustrated in Fig. 2. More details about the knuckle crease segmentation (tracing) and matching are elucidated in the subsequent subsections.

2.1 Knuckle localization

Since the primary focus of the paper is skin crease segmentation of knuckle images, we need an effective strategy to localize the knuckle regions. To meet this need, we use the knuckle localization procedure of [10], as this work is established to provide accurate localization both in terms of the bounding box regression and the centroid detection. The knuckle localization approach developed by our team in [10] was derived from the capabilities of single-stage and two-stage deep-learning-based object detectors. In view of the observation that no single detector yields notable localization

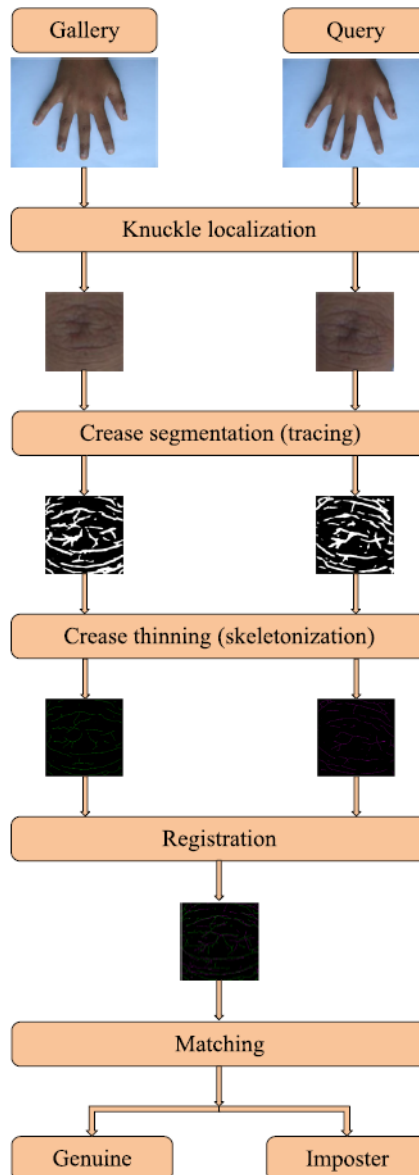


Fig. 1 Overall block diagram

results for the knuckle images with diverse backgrounds, orientations, and illumination conditions, this method considers ensembling of the single-stage and two-stage object detectors for generalized knuckle localization in varying conditions. The you-only-look-once (YOLO) class of single-stage detectors and region-based convolutional neural networks (RCNN) as two-stage detectors were combined through weighted box

fusion strategy to obtain generalized and more accurate bounding boxes. The technique in [10] was also tested for cross-dataset evaluation and was demonstrated as effective with multiple datasets.

2.2 Ground truth preparation

To facilitate the deep learning models with adequate training, a ground truth is prepared for the task of knuckle crease segmentation. The segmentation ground truth is prepared by performing manual labeling of the knuckle creases by tracing them in a piece-wise linear way. A sample showing preparation of the ground truth are illustrated in Fig. 2, where the original knuckle image (left) and the corresponding annotations overlaid on the image (right) are displayed. The *ImageLabelor* app of MATLAB is used to obtain this ground truth. The binary ground truth crease map is created by tracing the annotations and dilating the lines with empirically fixed width of 3 pixels.

2.3 Knuckle segmentation

Segmentation is a more challenging problem in comparison to the localization. The knuckle segmentation deals with the tracing of the skin creases formed in the knuckle images. This paper investigates efficient segmentation models, including UNet [11], feature Pyramid network (FPN) [12, 13], Pyramid Scene Parsing Network (PSPNet) [14], DeepLabV3+ [15], UNet++ [16] and provides a numerical comparison for the knuckle crease segmentation. These models are selected in view of their exemplary performances for the semantic segmentation task [17]. All these models possess exclusive characteristics to support adequate segmentation. For instance, UNet has an encoder-decoder architecture which comprises of symmetrical contracting and expanding paths to capture the context and localize precisely. The FPN architecture consists of multi-scale hierarchy of deep convolution networks which can produce the feature pyramids facilitating high-level semantic feature maps at all scales. PSPNet utilizes a pyramid pooling module which can exploit the global context information through aggregation of contexts from local regions. DeepLabV3+ attempts to combine the advantages of both the spatial pyramid pooling module and the encoder-decoder structure in terms of encoding multiscale contextual information and capturing sharper object boundaries, respectively. UNet++ deals with minimizing the semantic gap between the feature maps of encoder and decoder by introducing a series of nested dense skip pathways between the sub-networks.

2.4 Matching

There has been no established work to match knuckle images through their crease maps. In the current work, we focus on deriving the matching score through the predicted centerline crease maps of the knuckle regions. The matching score is obtained through the proposed registered crease quality (RCQ) descriptor. The segmentation procedure described in Sect. 2.2 is evaluated with multiple potential performance metrics, where centerline metrics is the one category to indicate the effectiveness of the segmentation procedure with respect to the ground truth centerlines allowing a reasonable distance threshold δ (as specified in Sect. 3.3). Among the centerline

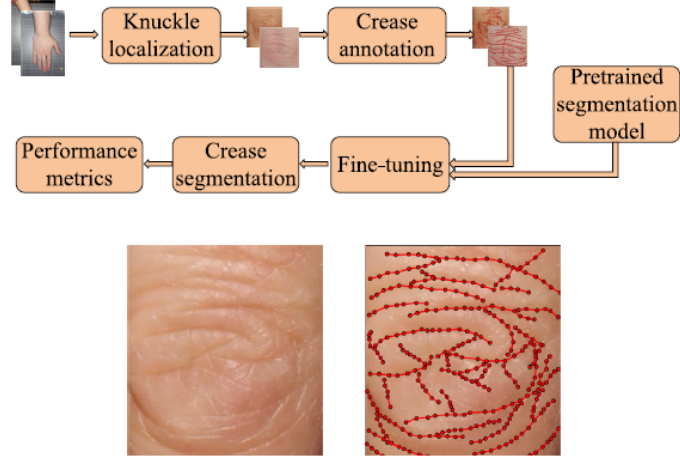


Fig. 2 (top) Crease segmentation procedure, (bottom-left) Sample knuckle image, (bottom-right) Overlaid manual annotations

metrics (refer to Eqs. (2–4) in Sect. 3.3), quality is a more general metrics combining correctness and completeness. For the segmentation accuracy, the quality metric is measured with the ground truth as the reference. On the other hand, the measurement of registered crease quality (RCQ) is furnished with the same formulae (of Eqs. (2–4)) but considering the gallery image as the reference. Hence, the RCQ metric yields a matching score between the gallery image and registered query image.

In this descriptor, the quality metric of the predicted centerlines is obtained after performing the registration between the query and the gallery image. The registration step furnishes the geometric transformation estimated from the gallery and the query images (termed as the reference and sensed images in the related nomenclature) [18]. Owing to its capabilities of multiview, multitemporal and multimodal analyses [18], the registration step facilitates the aligning of knuckles. This aligning allows for overlap of the creases and the pixel-wise comparison helps in determining a match or no match.

Figure 3 illustrates the process of the proposed RCQ descriptor for a query and gallery image belonging to the same subject. The first two columns of the figure show the gallery and query images, respectively, with their predicted masks and the corresponding centerlinemaps in middle and the bottom rows. The third column demonstrates that if we try to find the quality between the query and gallery images without any preprocessing, the score is likely to be extremely low because it leads to poor correspondence between the pixels belonging to the knuckle creases. However, the registration step can make the query image align with the gallery image if they both belong to the same subject (genuine pairs), and there will be practically no impact if the two images belong to different subjects (imposter pairs). Therefore, values of the quality metric will shoot up as a result of registration between the genuine pairs whilst keeping them unaffected for the imposter pairs. Consequently, the separation between the genuine and imposter scores would also increase turning into better distinguishing ability and recognition accuracy. The fifth column of Fig. 3 highlights the impact of registration on increasing the chances of a correct match.

3 Experiments and results

This section presents the details about the datasets used, the training–testing strategy, performance metrics and numerical results.

3.1 Dataset

Looking at the importance of the crease segmentation task and its subjection to the pronounced visibility of deep creases, we work with an in-house high-quality hand dorsal dataset named as **H-Unique high quality (HUQ-HQ)** dataset to train and evaluate the segmentation models. This dataset is acquired with a Canon EOS 5DS R digital single-lens reflex (DSLR) camera and it offers high-resolution images of the order of 8688×5792 pixels. The **HUQ-HQ dataset** contains hand dorsal images of the left and right hands of 66 subjects, leading to 132 distinct classes. The database has equal contributions from male and female participants of diverse age groups and ethnicities. A sample image from the **HUQ-HQ** dataset is shown in Fig. 4(left). The knuckle regions from the hand dorsal images of 50 subjects are extracted using the ensemble approach [10]. Further, the manual annotations of knuckle creases from 50 images of PIP knuckles from the HUQ-HQ dataset are obtained as explained in Section 2.1. These manual annotations are then stored in the form of binary creasemaps, so that they can be utilized for training of the segmentation model. Some knuckle images and their corresponding annotations and centerline maps are illustrated in Fig. 5.

For the evaluation purposes, another public hand dorsal dataset named as the **PolyU Hand Dorsal (HD)** dataset is employed. This dataset comprises of full hand dorsal images from 502 subjects, where resolution of each image is 1600×1200 . This dataset is more generalized in terms of the skin-color and hand orientations. The paper uses the **HD dataset** for the evaluation of crease-matching only. The matching experiments are conducted with the PIP knuckles of middle finger only, coming from the first 200 subjects of the **HD dataset** and five samples of each subject. Hence, the matching investigations are conducted with 1000 knuckle images in total. A sample image from the HD dataset is depicted in Fig. 4(right).

3.2 Experimental setup

The segmentation models are fine-tuned with the pairs of knuckle images and corresponding annotated crease maps [19]. The segmentation models are initialized with the weights obtained with ImageNet dataset [20], and fine tuning is performed with the Adam optimizer for 40 epochs with initial learning rate of 0.0001 which is further decreased to 0.00001 after 25th epoch [19]. The data is augmented with horizontal flip, blur, random crop, affine and perspective transforms to enrich the training set. Furthermore, five pairs of knuckle image and corresponding crease maps are used for validation and testing.

3.3 Performance metrics

We evaluate the model’s performance in terms of the segmentation and its matching ability. To evaluate and compare the segmentation performance, we calculate the

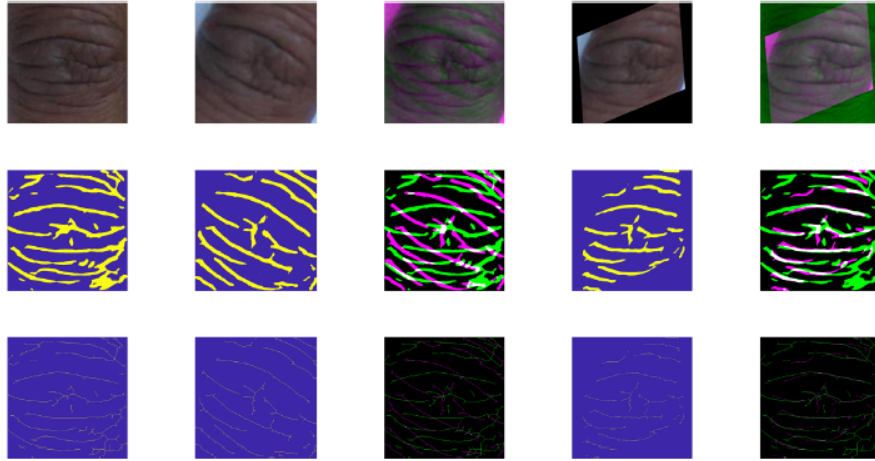


Fig. 3 Effect of map registration over centerline creases, (top row)RGB image, (middle row) Predicted crease map, (bottom row) Centerline of the predicted map; (1st col.) Gallery image, (2nd col.) Query image, (3rd col.) Overlaying of images from cols. 1 and 2, (4th col.) Registered query image, (5th col.) Overlaying of images from cols. 1 and 4

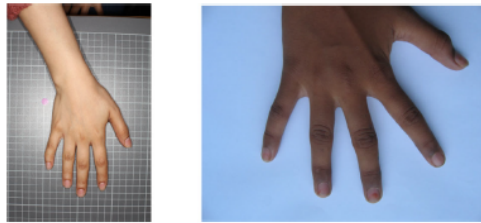


Fig. 4 Sample images; (left) HUQ-HQ, (right) HD dataset

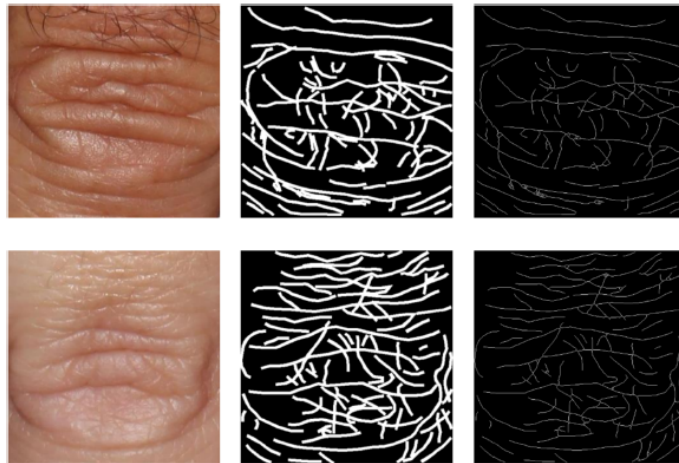


Fig. 5 Sample images; (left) Extracted knuckles, (middle) Corresponding annotated crease maps, (right) Centerline maps

intersection over union (IoU), F1 score, sensitivity, specificity and negative predictive values (NPV). The mathematical definition of various metrics are furnished below:

$$\begin{aligned}
IoU &= \frac{TP}{TP + FP + FN} \\
F1 &= \frac{2TP}{2TP + FP + FN} \\
Sens &= \frac{TP}{TP + FN} \\
Spec &= \frac{TN}{TN + FP} \\
NPV &= \frac{TN}{TN + FN}
\end{aligned} \tag{1}$$

where TP, FP, TN, FN represent the true positives, false positives, true negatives and false negatives respectively. TP are the pixels that belong to the crease and are predicted as the crease. FP are the pixels that belong to the background and are predicted as the crease. TN are the pixels that belong to the background and are predicted as the background. FN are the pixels that belong to the crease and are predicted as the background.

Centerline performance metrics are employed for a more thorough evaluation. The advantage of using knuckle predictions as centerlines is to eradicate the varied thickness of the crease predictions made from different models. By doing so, we can calculate the completeness (Comp), correctness (Corr) and quality (Qual) of the predicted crease centerlines [21] of the predicted centreline (Pr) against the ground truth centreline (GT). The completeness explains howcomplete is the predicted crease map or how much is missing in the map [22]. Whereas, correctness is related to the probability of a predicted crease to be indeed a crease [22]. The definitions of centerlinemetrics can be made clearer from Fig. 6 The completeness can be defined as ratio of length ofmatched ground truth to the total length of ground truth. On the other hand, correctness can be expressed as length ofmatched prediction to the total length of prediction.

$$Comp = \frac{|\mu_{Pr}(GT)|}{|GT|} \tag{2}$$

$$Corr = \frac{|\mu_{GT}(Pr)|}{|Pr|} \tag{3}$$

$$Qual = \frac{|\mu_{GT}(Pr)|}{|Pr| + |GT| - |\mu_{Pr}(GT)|} \tag{4}$$

where $\mu_A(B) = \{a \in A | b \in B, d(a, b) < \delta\}$ is the set of points of A with a corresponding point in B within reasonable distance d which is smaller than the buffer threshold δ . We set δ to 3 to allow a very small margin of error in the annotation or prediction of crease centrelines.

The completeness is the percentage of the ground truth datawhich is explained by the predicted data i.e., the percentage of the ground truth creases which lie within the buffer around the predicted creases. On the other hand, the correctness represents the percentage of correctly predicted creases i.e., percentage of the predicted creases

which lie within the buffer around the ground truth creases. In addition to the above, it is pertinent to know that the buffer is created by an empirically chosen threshold (δ), as depicted in eqs. (2–4) of the manuscript. The same has now been incorporated in the revised version of the manuscript.

The parameter δ is a distance threshold used to accommodate the potential shifts in centerline positions by relaxing the notion of a true positive from being a precise coincidence of points. This parameter is also referred to as the “buffer width” in the literature, which is there to consider the expected accuracy of the crease prediction algorithm. If its value is set too large, false extractions close to the actual knuckle crease will incorrectly be considered as crease. On the other hand, if its value is too small, correct crease predictions which are only slightly geometrically incorrect will be rejected. This is the reason the proposed work selects the value of parameter δ empirically (which is 3 for our experimentations).

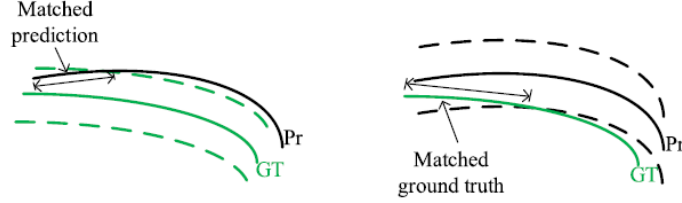


Fig. 6 Pictorial definitions of matched prediction and ground truth for calculation of centerline metrics

Table 1 Numerical results for segmentation models

Model (backbone)	Segmentation metrics					Centerline metrics		
	IoU	Sens.	Spec.	F1	NPV	Corr	Comp	Qual
UNet (mobilenet-v2)	0.40	0.51	0.86	0.57	0.78	0.64	0.57	0.42
FPN (densenet121)	0.33	0.45	0.83	0.50	0.75	0.59	0.31	0.25
PSPnet (efficientnet-b3)	0.35	0.50	0.84	0.52	0.80	0.63	0.45	0.35
DeepLabV3+ (resnet152)	0.41	0.53	0.86	0.58	0.80	0.64	0.56	0.42
UNet++ (densenet201)	0.42	0.63	0.85	0.59	0.88	0.71	0.62	0.49

3.4 Segmentation results

This paper constitutes the first work on segmentation of knuckle creases. There have been numerous works on knuckle recognition which usually build on black-box methods (like CNN based) or traditional feature extractors from the knuckle image as a whole. No existing work employs the segmented creases explicitly for establishing the identifiability of knuckles, which has been a bottleneck. Hence, through this paper we target on segmenting the knuckle creases in a precise manner using semantic segmentation techniques.

The performance metrics and sample crease segmentation for various models are presented in Table 1 and Fig. 7, respectively. The figure depicts the sample knuckle test image along with the ground truth of knuckle creases in the top row. While the bottom row constitutes the crease predictions from various segmentation models. It can be observed from the prediction masks that the mask pertaining to the model UNET++ is demonstrated to be the most accurate and most close to the ground truth, among all the predicted masks. A similar inference can be deduced from the metrics presented in Table 1, where bold entries indicate the best values of the employed metrics. The model UNET++ exhibits the highest IoU (0.42) and F1 value (0.59) as compared to the other models. Concurrently, the centerline metrics for UNET++ also outperform those of the other segmentation models. This clearly point towards choosing the UNET++ model over the other models for the rest of the segmentation and matching experiments.

The expert anthropologist played a crucial role in validating the segmentation results by providing anatomical insights into the correctness of the segmented creases. Specifically, she reviewed the alignment, continuity, and anatomical relevance of the detected features (such as creases and centerlines) based on her expertise.

Not only has the anthropologist ensured the anatomical relevance through consistent feedback at the time of knuckle crease annotation, but she also provided the critical feedback about the predictions made with the test cases. One such sample of expert feedback is depicted below in Fig. 8, where the anthropologist has marked the regions where the predictions exhibit strong mismatch with the anatomical knuckle creases. The figure illustrates certain region in the top-left of the predicted image in the middle, where a crease has been predicted despite of having no crease as is evident from the anthropologist’s feedback on the right. This spurious prediction is probably due to the background shadow. Other highlighted regions indicate the instances where the model misses few shallow creases as observed in the anthropologist’s feedback on the right. Hence, this qualitative assessment is used to corroborate the quantitative metrics (segmentation and centerline metrics) reported in the study. This dual evaluation ensured that the results were both anatomically meaningful and computationally accurate.

Table 2 Comparison of performance metrics

Approach	EER (%)	AUC	DI
DenseNet	20.94	0.8665	1.3952
ResNet	21.90	0.8651	1.3310
Vgg19	24.65	0.8271	1.1651
AlexNet	22.90	0.8513	1.2736
Proposed	12.82	0.9273	2.1563

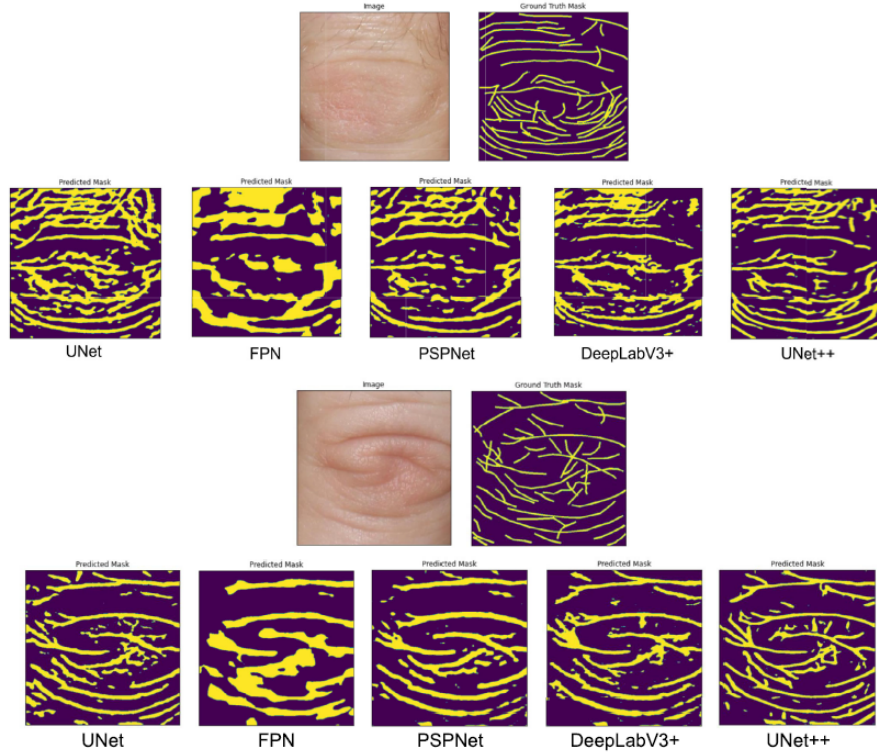


Fig. 7 Segmentation results for sample test images

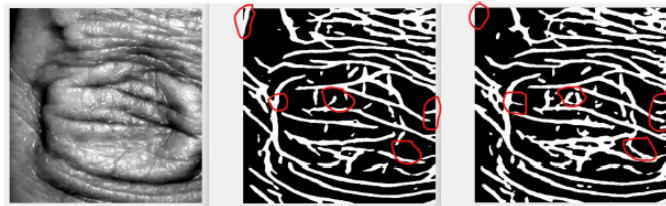


Fig. 8 Example of feedback from the anthropologist; (left)Knuckle image; (middle) predicted knuckle creases, (right) feedback from anthropologist

3.5 Matching results

For the matching experiment, current work utilizes a subset of the PolyU Hand Dorsal (HD) dataset [23], which comprises of extracted knuckle regions from the proximal interphalangeal (PIP) joints or the major knuckles [10] of the middle fingers from five different samples of right hands of 200 subjects. It is worth mentioning that the extractions are derived from the ensemble-based knuckle localization method proposed by Vyas et al. [10]. Hence, there are 1000 knuckle images constituted in this subset, and each knuckle image is resized to have the fixed dimension of 512×512 . The matching is performed by comparing each image of the database against every other

image. This one-to-all matching approach generates $N \times \binom{t}{2}$ genuine and $\binom{N}{2} \times t^2$ imposter scores for N subjects and t samples per subject. In total, this leads to leading to a total of 2000 genuine and 497,500 imposter scores.

The matching experiment has resulted in promising performance which is reflected through the low value of equal error rate (EER) and high value of area under the receiver operating characteristics (ROC) curves (AUC) and decidability index (DI) [2]. The respective values of these metrics are found to be 12.82%, 0.9273 and 2.1563. The corresponding ROC curve is presented in Fig. 9(right). The performance of the proposed approach is compared against multiple pretrained VGG19 and AlexNet convolutional neural network (CNN) models, which have been in use in recently reported works [24, 25] respectively. The ROC curves clearly indicate that the proposed RCQ descriptor outperforms these state-of-the-art models by a huge margin. Concurrently, other efficient pre-trained CNN models like DenseNet201 [26] and ResNet101 [27] are also employed in the comparison to make it more comprehensive. It is worth specifying that the CNN-based matching experiments were conducted using cosine-distance function. Nevertheless, the proposed matching algorithm emerges as the best performer in terms of the EER, AUC and DI, as is evident from the ROC of Fig. 9 and values presented in Table 2, where bold entries indicate the best values of the employed metrics.

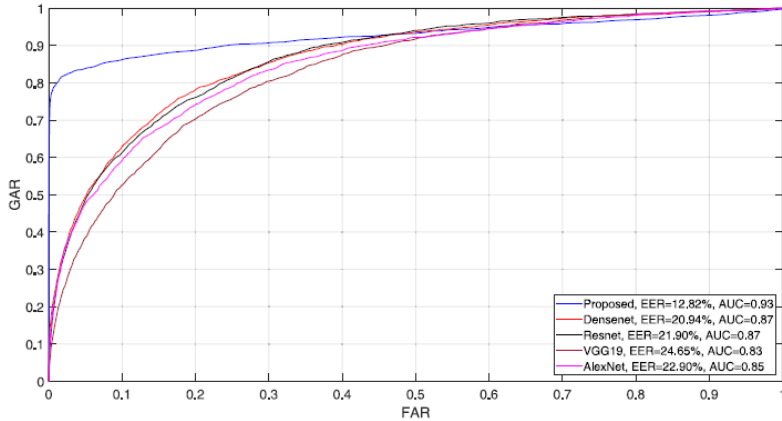


Fig. 9 ROC curves for the matching experiment

4 Conclusion

This paper presents a first-of-its-kind knuckle comparison through the segmentation of the knuckle creases. The paper facilitates a demonstrable and reproducible knuckle matching procedure, which strengthens its potential to act as evidence to support court-room proceedings. The paper explores the potential of segmenting knuckle creases, a task which remains under-explored by the research community so far. This

task is accomplished through fine tuning of the segmentation models with ground truth crease annotations, and exclusive performance analysis of the crease maps and their corresponding centerline maps. The paper recommends the best model for the crease segmentation task, which happens to be UNet++. In addition to the above, the paper investigates the identification ability of the knuckle creases with a public dataset and exhibits outperforming results. The matching procedure, being demonstrable, anatomy driven and reproducible, is deemed to be appropriate for the forensic applications. The EER can further be improved by incorporating knuckle crease features from diverse knuckle regions like major (or proximal inter-phalangeal (PIP)), minor (or distal interphalangeal (DIP)) and base (meta carpophalangeal). However, annotating the base knuckles is highly subjective, mainly because of the presence of large number of skin creases in that area making it difficult to annotate the knuckle creases precisely. Nevertheless, this research direction will prove to be a potential avenue for the knuckle crease segmentation problem.

Author Contributions

Conceptualization, B.M.W. and R.V.; methodology, B.M.W. and R.V.; software, R.V.; validation, B.M.W., H.R., R.V., and Z.J.; formal analysis, R.V. and B.M.W.; investigation, R.V. and B.M.W.; resources, B.M.W. and R.V.; data curation, R.B.-C., B.M.W., and R.V.; writing-original draft preparation, R.V.; writing-review and editing, B.M.W., H.R., and S.B.; visualization, B.M.W.; supervision, B.M.W., H.R., and P.A.; project administration, B.M.W. and S.B.; and funding acquisition, S.B. All authors have read and agreed to the published version of the manuscript.

Funding

The work in this publication is supported by funding from the European Research Council (ERC) under the European Union’s Horizon 2020 research and innovation programme (grant agreement No 787768).

Data Availability

The public hand databases 11k and HD are respectively available at: <https://sites.google.com/view/11khands> (accessed on 21 December 2021) and <http://www4.comp.polyu.edu.hk/~csajaykr/knuckleV2.htm> (accessed on 21 December 2021). The proprietary HUQ database (which is specifically collected under the H-Unique project) is still under collection.

5 Declarations

5.1 Conflict of interest

The authors declare no conflict of interest.

5.2 Ethics approval and consent to participate

The study was conducted according to the guidelines of the Declaration of Helsinki, and approved by the Faculty of Health and Medicine Research Ethics Committee (FHMREC) of Lancaster University (FHMREC Reference: FHMREC18001, dated 5 October 2018). Informed consent was obtained from all subjects involved in the study.

5.3 Consent for publication

Not applicable.

5.4 Materials availability

Not applicable.

5.5 Code availability

Not applicable.

References

- [1] Jaswal, G., Kaul, A., Nath, R.: Knuckle print biometrics and fusion schemes—overview, challenges, and solutions. *ACM Computing Surveys (CSUR)* **49**(2), 1–46 (2016)
- [2] Vyas, R., Rahmani, H., Boswell-Challand, R., Angelov, P., Black, S., Williams, B.M.: Robust end-to-end hand identification via holistic multi-unit knuckle recognition. In: *2021 IEEE International Joint Conference on Biometrics (IJCB)*, pp. 1–8 (2021). IEEE
- [3] Kumar, A., Zhou, Y.: Human identification using knucklecodes. In: *2009 IEEE 3rd International Conference on Biometrics: Theory, Applications, and Systems*, pp. 1–6 (2009). IEEE
- [4] Kumar, A., Zhou, Y.: Personal identification using finger knuckle orientation features. *Electronics Letters* **45**(20), 1023–1025 (2009)
- [5] Zhang, L., Zhang, L., Zhang, D., Zhu, H.: Online finger-knuckle-print verification for personal authentication. *Pattern recognition* **43**(7), 2560–2571 (2010)
- [6] Zhang, L., Zhang, L., Zhang, D., Zhu, H.: Ensemble of local and global information for finger-knuckle-print recognition. *Pattern recognition* **44**(9), 1990–1998 (2011)
- [7] Cheng, K., Kumar, A.: Contactless finger knuckle identification using smart-phones. In: *2012 BIOSIG-proceedings of the International Conference of Biometrics Special Interest Group (BIOSIG)*, pp. 1–6 (2012). IEEE

- [8] Kumar, A., Wang, B.: Recovering and matching minutiae patterns from finger knuckle images. *Pattern Recognition Letters* **68**, 361–367 (2015)
- [9] Edmond, G.: Pathological science? demonstrable reliability and expert forensic pathology evidence. *Demonstrable Reliability and Expert Forensic Pathology Evidence* (March 11, 2008). UNSW Law Research Paper (2008-6) (2008)
- [10] Vyas, R., Williams, B.M., Rahmani, H., Boswell-Challand, R., Jiang, Z., Angelov, P., Black, S.: Ensemble-based bounding box regression for enhanced knuckle localization. *Sensors* **22**(4), 1569 (2022)
- [11] Ronneberger, O., Fischer, P., Brox, T.: U-net: Convolutional networks for biomedical image segmentation. In: *Medical Image Computing and Computer-assisted intervention—MICCAI 2015: 18th International Conference, Munich, Germany, October 5–9, 2015, Proceedings, Part III 18*, pp. 234–241 (2015). Springer
- [12] Lin, T.-Y., Dollár, P., Girshick, R., He, K., Hariharan, B., Belongie, S.: Feature pyramid networks for object detection. In: *Proceedings of the IEEE Conference on Computer Vision and Pattern Recognition*, pp. 2117–2125 (2017)
- [13] Kirillov, A., He, K., Girshick, R., Dollár, P.: A unified architecture for instance and semantic segmentation. In: *Computer Vision and Pattern Recognition Conference* (2017). CVPR
- [14] Zhao, H., Shi, J., Qi, X., Wang, X., Jia, J.: Pyramid scene parsing network. In: *Proceedings of the IEEE Conference on Computer Vision and Pattern Recognition*, pp. 2881–2890 (2017)
- [15] Chen, L.-C., Zhu, Y., Papandreou, G., Schroff, F., Adam, H.: Encoder-decoder with atrous separable convolution for semantic image segmentation. In: *Proceedings of the European Conference on Computer Vision (ECCV)*, pp. 801–818 (2018)
- [16] Zhou, Z., Rahman Siddiquee, M.M., Tajbakhsh, N., Liang, J.: Unet++: A nested u-net architecture for medical image segmentation. In: *Deep Learning in Medical Image Analysis and Multimodal Learning for Clinical Decision Support: 4th International Workshop, DLMIA 2018, and 8th International Workshop, ML-CDS 2018, Held in Conjunction with MICCAI 2018, Granada, Spain, September 20, 2018, Proceedings 4*, pp. 3–11 (2018). Springer
- [17] Everingham, M., Eslami, S.A., Van Gool, L., Williams, C.K., Winn, J., Zisserman, A.: The pascal visual object classes challenge: A retrospective. *International journal of computer vision* **111**, 98–136 (2015)
- [18] Zitova, B., Flusser, J.: Image registration methods: a survey. *Image and vision computing* **21**(11), 977–1000 (2003)

- [19] Yakubovskiy, P.: Segmentation Models Pytorch. GitHub (2020)
- [20] Deng, J., Dong, W., Socher, R., Li, L.-J., Li, K., Fei-Fei, L.: Imagenet: A large-scale hierarchical image database. In: 2009 IEEE Conference on Computer Vision and Pattern Recognition, pp. 248–255 (2009). Ieee
- [21] Mosinska, A., Marquez-Neila, P., Koziński, M., Fua, P.: Beyond the pixel-wise loss for topology-aware delineation. In: Proceedings of the IEEE Conference on Computer Vision and Pattern Recognition, pp. 3136–3145 (2018)
- [22] Wiedemann, C., Heipke, C., Mayer, H., Jamet, O.: Empirical evaluation of automatically extracted road axes. *Empirical evaluation techniques in computer vision* **12**, 172–187 (1998)
- [23] Kumar, A., Xu, Z.: Personal identification using minor knuckle patterns from palm dorsal surface. *IEEE Transactions on Information Forensics and Security* **11**(10), 2338–2348 (2016)
- [24] Tarawneh, A.S., Hassanat, A.B., Alkafaween, E., Sarayrah, B., Mnasri, S., Altarawneh, G.A., Alrashidi, M., Alghamdi, M., Almuhaimeed, A.: Deepknuckle: deep learning for finger knuckle print recognition. *Electronics* **11**(4), 513 (2022)
- [25] Heidari, H., Chalechale, A.: Biometric authentication using a deep learning approach based on different level fusion of finger knuckle print and fingernail. *Expert Systems with Applications* **191**, 116278 (2022)
- [26] Huang, G., Liu, Z., Van Der Maaten, L., Weinberger, K.Q.: Densely connected convolutional networks. In: Proceedings of the IEEE Conference on Computer Vision and Pattern Recognition, pp. 4700–4708 (2017)
- [27] He, K., Zhang, X., Ren, S., Sun, J.: Deep residual learning for image recognition. In: Proceedings of the IEEE Conference on Computer Vision and Pattern Recognition, pp. 770–778 (2016)